


# [8]-Gingerol exerts anti-myocardial ischemic effects in rats via modulation of the MAPK signaling pathway and L-type $\text{Ca}^{2+}$ channels

Yucong Xue<sup>1</sup> | Muqing Zhang<sup>1,2</sup> | Bin Zheng<sup>3</sup> | Yuanyuan Zhang<sup>3</sup> | Xi Chu<sup>4</sup> | Yu Liu<sup>3</sup> | Ziliang Li<sup>5</sup> | Xue Han<sup>3,6</sup> | Li Chu<sup>3,7</sup> 

<sup>1</sup>College of Integrative Medicine, Hebei University of Chinese Medicine, Shijiazhuang, Hebei, China

<sup>2</sup>Affiliated Hospital, Hebei University of Chinese Medicine, Shijiazhuang, Hebei, China

<sup>3</sup>School of Pharmacy, Hebei University of Chinese Medicine, Shijiazhuang, Hebei, China

<sup>4</sup>The Fourth Hospital of Hebei Medical University, Shijiazhuang, Hebei, China

<sup>5</sup>School of Basic Medicine, Hebei University of Chinese Medicine, Shijiazhuang, Hebei, China

<sup>6</sup>Hebei Higher Education Institute Applied Technology Research Center on TCM Formula Preparation, Shijiazhuang, Hebei, China

<sup>7</sup>Hebei Key Laboratory of Chinese Medicine Research on Cardio-Cerebrovascular Disease, Shijiazhuang, Hebei, China

## Correspondence

Li Chu and Xue Han, School of Pharmacy, Hebei University of Chinese Medicine, 3 Xingyuan Road, Shijiazhuang, Hebei 050200, China.

Email: chuli0614@126.com; hanxuecc@126.com

Ziliang Li, School of Basic Medicine, Hebei University of Chinese Medicine, 3 Xingyuan Road, Shijiazhuang, Hebei 050200, China.

Email: liziliang321@126.com

## Funding information

The Project of Science and Technology Research Project of Hebei Province, Grant/Award Number: BJ2020002; The Excellent Youth Program of Hebei University of Chinese Medicine, Grant/Award Number: YQ2020003

## Abstract

Myocardial ischemia (MI) remains the leading cause of mortality worldwide. Therefore, it is urgent to seek the treatment to protect the heart. [8]-Gingerol (8-Gin), one of the most active ingredients in ginger, has antioxidant, cardiogenic, and cardiovascular protective properties. The present study elucidated the cardioprotection effects and underlying mechanisms of 8-Gin in isoproterenol (ISO)-induced MI. ISO (85 mg/kg/d) was subcutaneously injected for 2 consecutive days to induce acute MI model in rats. Electrocardiography, oxidative stress levels, calcium concentrations, and apoptosis degree were observed. The effects of 8-Gin on L-type  $\text{Ca}^{2+}$  current ( $I_{\text{Ca-L}}$ ), contraction, and  $\text{Ca}^{2+}$  transients were monitored in rat myocytes via patch-clamp and IonOptix detection systems. 8-Gin decreased J-point elevation and heart rate and improved pathological heart damage. Moreover, 8-Gin reduced the levels of CK, LDH, and MDA, ROS production, and calcium concentrations in myocardial tissue, while increased the activities of SOD, CAT, and GSH. In addition, 8-Gin down-regulated Caspase-3 and Bax expressions, while up-regulated Bcl-2 expression. 8-Gin produced a marked decrease in the expression of p38, JNK, and ERK1/2 proteins. 8-Gin inhibited  $I_{\text{Ca-L}}$ , cell contraction, and  $\text{Ca}^{2+}$  transients in isolated rat myocytes. The results

**Abbreviations:** [ $\text{Ca}^{2+}$ ]<sub>i</sub>, intracellular  $\text{Ca}^{2+}$ ; 8-Gin, [8]-gingerol; CAD, coronary artery disease; CON, the control group; ECG, electrocardiogram; ERK1/2, extracellular regulated kinase; H-8-Gin, high-dose 8-Gin group;  $I_{\text{Ca-L}}$ , L-type  $\text{Ca}^{2+}$  current; ISO, isoproterenol; JNK, c-jun N-terminal kinase; L-8-Gin, low-dose 8-Gin group; LTCCs, the L-type  $\text{Ca}^{2+}$  channels; MAPK, mitogen-activated protein kinase; MI, myocardial ischemia; Nic, nicardipin; ROS, reactive oxygen species; SR, sarcoplasmic reticulum; VER, verapamil.

Yucong Xue and Muqing Zhang contributed equally to this work.

This is an open access article under the terms of the Creative Commons Attribution-NonCommercial-NoDerivs License, which permits use and distribution in any medium, provided the original work is properly cited, the use is non-commercial and no modifications or adaptations are made.

© 2021 The Authors. *Pharmacology Research & Perspectives* published by British Pharmacological Society and American Society for Pharmacology and Experimental Therapeutics and John Wiley & Sons Ltd.

indicate that 8-Gin could exert anti-myocardial ischemic effects, which may be associated with oxidative stress reduction, cardiomyocytes apoptosis inhibition through MAPK signaling pathway, and  $\text{Ca}^{2+}$  homeostasis regulation via  $I_{\text{Ca-L}}$  modulation.

#### KEYWORDS

[8]-gingerol, cell contractility, L-type  $\text{Ca}^{2+}$  current, MAPK signaling pathway, myocardial ischemia, oxidative stress

## 1 | INTRODUCTION

Ginger, the fresh root of *Zingiber officinale* Roscoe, has an aromatic and spicy flavor. As a kind of medicinal and edible plant, it is widely cultivated worldwide.<sup>1</sup> Gingerol is a pungent substance containing phenolic functional groups and is found naturally in raw ginger materials. However, due to different substituents, benzene ring positions, and side chain length, many different gingerols, such as [6]-, [8]-, and [10]-gingerol,<sup>2</sup> are formed. [8]-Gingerol (8-Gin) is provided with antioxidant, anti-inflammatory, cardiogenic, and cardiovascular protective properties.<sup>3-5</sup> The chemical structure of 8-Gin is shown in Figure 1. Coronary artery disease (CAD) refers to coronary atherosclerosis caused by vascular lumen stenosis or obstruction and coronary artery function changes, which causes myocardial ischemia (MI), hypoxia, or necrosis.<sup>6</sup> Although there are multiple therapies recently, MI remains the leading cause of mortality worldwide.<sup>7</sup> Although 8-Gin has many beneficial pharmacological properties, its protective effects on MI and potential mechanisms have not yet been explored.

Previous study demonstrated that cardiomyocytes ischemic injury was related to reactive oxygen species (ROS), which produced during tissue ischemia, caused oxidative stress in cardiomyocytes, and further led to apoptosis.<sup>8</sup> Furthermore, ROS production also causes activation of many intracellular signaling pathways, one of which is the mitogen-activated protein kinase (MAPK) pathway.<sup>9</sup> The MAPK family plays a key role in cell growth, disease occurrence, and development. The MAPK signaling pathway has three subfamilies of stress kinases: p38, c-jun N-terminal kinase (JNK), and extracellular regulated kinase (ERK1/2). Studies demonstrated that p38 and JNK induced inflammation and apoptosis, and ERK1/2 regulated differentiation and proliferation, promoted cell survival, and protected cardiomyocytes.<sup>10,11</sup> Previous research suggested that these kinases eventually induced caspase activation through

different transcription mechanisms.<sup>12</sup> More often, caspases can be activated by mitochondrial-related proteins, which were mediated by the Bcl-2 family proteins.<sup>13</sup> Bcl-2 family proteins contain anti-apoptotic genes Bcl-2 and apoptosis-stimulating protein Bax. Evidence has been found that the stress-activated JNK (p-JNK) mediates phosphorylation of Bcl-2 under ischemic conditions, which leads to irreversible cardiac injury.<sup>14</sup> Based on these studies, it appears that the level of ROS production and relative activity of MAPK pathway will determine whether cells survive or not. Therefore, this pathway may be a potential target for the therapy of MI disease by inhibition of oxidative stress and apoptosis.

It is well known that  $\text{Ca}^{2+}$  is a ubiquitous intracellular signal molecule responsible, which not only participate in cell signal transduction, protein expression and degradation, cardiomyocytes contraction, and diastole but also regulate cell survival and function.<sup>15,16</sup> Increasing evidence indicated that  $\text{Ca}^{2+}$  overload is also one of the most important mechanisms causing MI injury.<sup>17</sup>  $\text{Ca}^{2+}$  plays a crucial role in myocyte excitation-contraction coupling of heart. Previous studies have reported that intracellular  $\text{Ca}^{2+}$  ( $[\text{Ca}^{2+}]_i$ ) increasing or  $\text{Ca}^{2+}$  overload could increase cell contractility and then induce myocardial hypertrophy and apoptosis.<sup>18,19</sup> Moreover, recent research has shown that glycolysis, ROS production, and MI injury induce  $\text{Ca}^{2+}$  overload due to the decrease in calcium storage via the sarcoplasmic reticulum (SR).<sup>16</sup> Song et al. found that p38 MAPK pathway involved in the  $\text{Ca}^{2+}$  regulation. In isolated cardiomyocytes and perfused rat hearts, inhibition of p38 MAPK signaling reduced  $[\text{Ca}^{2+}]_i$  overload and attenuated suppressed apoptosis during the I/R process.<sup>20</sup> The L-type  $\text{Ca}^{2+}$  channels (LTCCs) comprise the main pathway of  $\text{Ca}^{2+}$  entry into myocardial cells. LTCCs blockers, such as verapamil (VER), generally have been verified to inhibit  $\text{Ca}^{2+}$  overload and show a cardioprotective effect during the process of MI.<sup>21</sup> Therefore, the maintenance of  $[\text{Ca}^{2+}]_i$  homeostasis is essential for the maintenance of cell physiological function. More importantly, drugs that can maintain  $[\text{Ca}^{2+}]_i$  homeostasis through inhibition of LTCCs are promising candidates for producing cardioprotective effects.<sup>22</sup>

In the present study, we ascertained the underlying cardioprotective mechanisms of 8-Gin on isoproterenol (ISO)-induced MI in rats. We investigated the effects of 8-Gin on oxidative stress, apoptosis, and MAPK signaling pathway and observed the influences of 8-Gin on L-type  $\text{Ca}^{2+}$  current ( $I_{\text{Ca-L}}$ ), cell contractility, and  $\text{Ca}^{2+}$  transients in rat ventricular myocytes. This series of experimental results may contribute to efforts to improve the efficacy of 8-Gin in clinical treatments and provide a new direction for the development of anti-MI drugs for clinical use in the future.

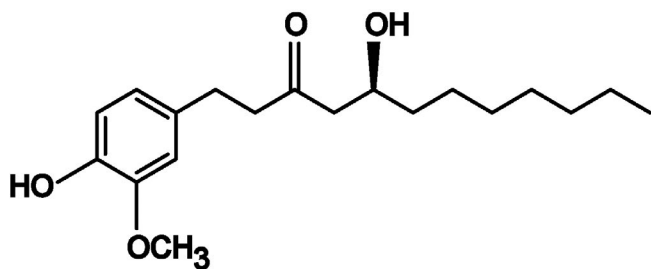


FIGURE 1 General structure of [8]-gingerol (8-Gin)

## 2 | MATERIALS AND METHODS

### 2.1 | Ethics statement

Original studies in animals have been carried out in accordance with the Guide for the Care and Use of Laboratory Animals as adopted and promulgated by the U.S. National Institutes of Health. The Animal Care and Ethical Committee of Hebei University of Chinese Medicine approved all animal protocols (approval number: DWLL2020073).

### 2.2 | Chemicals and animals

8-Gin was purchased from Chengdu Biopurify Phytochemicals Ltd. (Catalog: BP0108). ISO was purchased from Cayman Chemicals. Collagenase type II was purchased from GIBCO (Invitrogen). VER was purchased from Tokyo chemical industry Co., Ltd. When stated otherwise, other chemicals were purchased from Sigma-Aldrich. All solvents were of analytical grade and are commercially available.

Fifty adult male Sprague-Dawley (SD) rats (6–8 weeks,  $200 \pm 20$  g) were supplied by Hebei Medical University. All rats were bred in standard conditions (23–25°C and 40%–60% relative humidity with a 12 h light-dark cycle) with ad libitum availability of granular food and water.

### 2.3 | Experimental protocol

Fifty male rats (6–8 weeks,  $200 \pm 20$  g) were randomly separated into five groups ( $n = 10$  per group): (1) Control group (CON), (2) ISO group (ISO), (3) low-dose 8-Gin group (L-8-Gin), (4) high-dose 8-Gin group (H-8-Gin), and (5) VER group (VER). The CON group was given isovolumic normal saline. Groups of L- and H-8-Gin were injected intraperitoneally (i.p.) with 8-Gin (10 and 20 mg/kg/day).<sup>23,24</sup> The doses and route of administration of 8-Gin were chosen according to a previous study, which demonstrated that 30 mg/kg/day of 8-Gin given by i.p. exhibited significantly therapeutic effects in rats.<sup>24</sup> The VER group was injected intraperitoneally with VER (2 mg/kg/day).<sup>22,25</sup> For pretreatment with 8-Gin for 7 days, we first injected ISO (85 mg/kg/d) subcutaneously into all rats, except the CON group, for 2 consecutive days to establish an MI model.<sup>22,25</sup> After the end of the experiment, we used sodium pentobarbital (Sigma, 40 mg/kg, i.p.) to anesthetize rats, the heart was removed, and levels of relevant indicators were determined.

### 2.4 | Measurement of electrocardiogram and cardiac marker enzymes

After rats were anesthesia, we obtained the electrocardiogram (ECG) through the RM6240BD Biological Signal Collection System and

observed the change of heart rate and J-point in each group of rats. Rat sera were isolated by centrifugation, and the levels of creatinine kinase (CK) and lactate dehydrogenase (LDH) were detected using CK (Catalog: A032, Nanjing Jiancheng Bioengineering Institute) and LDH (Catalog: A020-2, Nanjing Jiancheng Bioengineering Institute) assay kits.

### 2.5 | Assessment of histopathological changes

We fixed heart specimens with 4% paraformaldehyde. After the specimen fixation, all tissue sections from each group were sectioned into 4- $\mu$ m-thick slices and stained with hematoxylin and eosin (H&E). Later, pathological changes in the heart were evaluated using a light microscope (Leica DM4000B). Image-Pro Plus software was used to calculate the percentage of positive signal staining area myocardial injury.

### 2.6 | Measurement of ROS

The fresh heart tissues were embedded with OCT embedding agent (Catalog: G6059-110ML, Servicebio technology Co., Ltd), and then sliced with a thickness of 8  $\mu$ m. The slices were incubated with ROS staining solution (Catalog: D7008, Sigma-Aldrich Chemicals, 1:500 dilution) in the dark at 37°C for half an hour. After incubation, we washed the slides three times with phosphate-buffered saline (PBS) for 5 min per wash. Next, a 4',6-diamidino-2-phenylindole (DAPI) staining solution (Catalog: G1012, Servicebio technology Co., Ltd) was added to the slices and counterstained for 10 min at room temperature. After that time, the sections were sealed with anti-fluorescence quenching encapsulant. Finally, we observed the changes in the sections using a fluorescence microscope (Leica DM4000B) and collected images.

### 2.7 | Determination of calcium concentration and oxidative stress markers

Rat heart tissue was prepared as a 10% homogenate. Myocardial calcium concentration was detected using the calcium kit (Rayto Life and Analytical Sciences Co., Ltd), according to the manufacturer's instructions. In addition, and according to the manufacturer's protocol, rat sera were isolated by centrifugation, and the activities of superoxide dismutase, catalase, and reduced glutathione (SOD, CAT, and GSH, respectively) and the content of malondialdehyde (MDA) were measured by assay kits for each enzyme (SOD, Catalog: A001-3, Nanjing Jiancheng Bioengineering Institute; CAT, Catalog: A007-1, Nanjing Jiancheng Bioengineering Institute; GSH, Catalog: A006-2-1, Nanjing Jiancheng Bioengineering Institute; and MDA, Catalog: A003-1, Nanjing Jiancheng Bioengineering Institute), respectively.

## 2.8 | Western blot analysis

Frozen cardiac specimens were weighed separately and homogenized in RIPA lysis buffer (Catalog: G2002, Servicebio technology Co., Ltd), then lysed for 30 min on ice. The homogenate was then centrifuged at 12,000g for 10 min at 4°C, the supernatant (total protein extract) was added to a precooled Eppendorf (EP) tube, and the protein concentration was measured using the bicinchoninic acid (BCA) protein assay kit (Catalog: G2026, Servicebio technology Co., Ltd). The protein samples were added to 10% sodium dodecyl polyacrylamide gels (SDS-PAGE) for electrophoresis (Millipore), and polyvinylfluoride (PVDF) membranes were selected to conduct protein transfer for 30 min on ice. After transferring the proteins, the membranes were added to a tube containing Tween and Tris-buffered saline buffer containing 5% non-fat milk, which was blocked for 30 min at room temperature. Next, the proteins were incubated with primary antibodies at 4°C overnight. The primary antibodies included anti-Bcl-2 (Catalog: PAA778Mu01, Cloud-Clone corp. Inc., 1:1000 dilution), anti-Bax (Catalog: GB11690, Servicebio technology Co., Ltd, 1:1000 dilution), anti-Caspase-3 (Catalog: 66470-2-Ig, Proteintech Group Inc., 1:1000 dilution), anti-p38 (Catalog: ab32142, Abcam, 1:1000 dilution), anti-JNK (Catalog: 24164-1-AP, Proteintech Group Inc., 1:1000 dilution), anti-ERK (Catalog: GB11560, Servicebio technology Co., Ltd, 1:1000 dilution), and anti- $\beta$ -actin (Catalog: GB12001, Servicebio technology Co., Ltd, 1:1000 dilution). Next, we incubated proteins with horseradish peroxidase (HRP)-conjugated secondary antibody (Catalog: GB23302, Servicebio technology Co., Ltd, 1:5000 dilution) for 30 min at 37°C. Finally, we scanned the film with a V370 (EPSON), and the bands' gray values were quantified using AlphaEaseFC software (Alpha Innotech).

## 2.9 | Isolation of ventricular myocytes

Male rat was injected with 500 IU/kg (i.p.) heparin for 20 min, and then sodium pentobarbital (40 mg/kg) was used to anesthetize the rat. After thoracotomy, the heart with a segment of aorta was quickly removed, and the residual blood in the heart was washed with frozen  $\text{Ca}^{2+}$ -free Tyrode's solution. After that, the heart was quickly hung on the Langendorff apparatus and poured with  $\text{Ca}^{2+}$ -free Tyrode's solution for 3 min. The digestive enzyme solution saturated with oxygen was then retrogradely perfused via the aorta at a constant rate of 6 ml/min for 20 min at 37°C until the heart became flaccid and pale. Next, the heart was removed from the Langendorff device, and the heart residual enzyme solution was washed out with 30 ml  $\text{Ca}^{2+}$ -free Tyrode's solution. Finally, the left ventricles were dissected into small pieces with ophthalmic scissors in oxygenated Krebs's solution, and the cardiomyocytes were maintained in Krebs's solution for more than 1 h at room temperature before the start of the experiment.

In terms of MI cells, we used ISO (85 mg/kg) to establish an MI model in which a rat was subcutaneously injected with ISO for 2 consecutive days. After that, the heart of myocardial ischemic rat

was removed and used for experiments with the same experimental protocols as described above.

## 2.10 | Recordings of $I_{\text{Ca-L}}$

The whole-cell patch clamp technique was used to record the  $I_{\text{Ca-L}}$  of isolated ventricular myocytes at room temperature (23–25°C). Glass patch electrodes with resistances of 3 to 5 M $\Omega$  were made using a pipette puller (Sutter Instrument). The Axon patch 700B amplifier was filtered at 2 kHz and used to record the current of calcium, and the results were analyzed by p-clamp 10.6 software (Axon Instruments). In experiments, series resistance compensation is controlled at 50%–70% extent.

## 2.11 | Measurement of myocytes contraction and $\text{Ca}^{2+}$ transients

The myocardial cells contraction and  $\text{Ca}^{2+}$  transients were measured using Ion Optix system (Ion Optix Corp.). The ventricular myocytes were allowed to settle onto the glass stage of an inverted microscope and gently flooded with a normal external Tyrode's solution. Cell contraction was triggered by field stimulation at 0.5 Hz frequency (2 ms duration per stimulation). Only rod-type shaped cardiomyocytes with clear margins and texture were selected to record contraction. Cardiomyocytes were incubated with the fluorescent indicator fura-2 AM (1 mM/L) for 15 min at room temperature in a photophobic environment.<sup>26</sup> The fluorescence intensity was measured with either a 340 or 380 nm filter (bandwidth  $\pm$  15 nm), and  $\text{Ca}^{2+}$  transients of myocytes were calculated based on fluorescence emission at 510 nm.<sup>27</sup>

## 2.12 | Data analysis

The data are given as the mean values  $\pm$  standard error of the mean (SEM). Statistical analyses were measured using one-way analysis of variance (ANOVA) followed by post hoc Bonferroni correction for multiple comparisons. The  $I_{\text{Ca-L}}$  data were analyzed using Clampfit 10.6 (Molecular Devices) and Origin 7.5 (OriginLab Corp.) statistical analysis software. The results were considered to be statistically significant at  $p$ -value  $<.05$  ( $p <.05$ ).

# 3 | RESULTS

## 3.1 | Effects of 8-Gin on ECG

As shown in Table 1, we observed that J-point was significantly elevated and heart rate was apparently increased in the ISO group ( $p <.01$ ). After pretreatment with 8-Gin, J-point and heart rate were both lower than in the ISO group ( $p <.05$  or  $<.01$ ).

TABLE 1 Effects of 8-Gin on electrocardiography

Group	J-point elevation (mV)	Heart rate (beats/min)
CON	0.022 ± 0.003	329.27 ± 11.89
ISO	0.042 ± 0.006**	476.92 ± 17.87**
L-8-Gin	0.027 ± 0.004 <sup>#</sup>	371.92 ± 16.35 <sup>##</sup>
H-8-Gin	0.019 ± 0.003 <sup>##</sup>	320.67 ± 9.81 <sup>##</sup>
VER	0.025 ± 0.004 <sup>#</sup>	322.31 ± 11.48 <sup>##</sup>

Data are presented as the mean ± SEM ( $n = 10$ ). \*\* $p < .01$  compared with the CON group; <sup>#</sup> $p < .05$  and <sup>##</sup> $p < .01$  compared with the ISO group. Statistical analyses were performed using one-way ANOVA followed by the Bonferroni correction.

### 3.2 | Effects of 8-Gin on myocardial enzymes and histopathology

Figure 2A,B showed the serum activities of CK and LDH were dramatically raised in the ISO group ( $p < .01$ ). After treatment of 8-Gin and VER, a distinct reduction in contrast to the ISO group ( $p < .01$ ) was found. Figure 2C,D showed no obvious tissue injury in the CON group. On the contrary, heart tissue in the ISO group manifested obvious myocardial cell swelling, inflammatory cell infiltration, apoptosis, and necrosis. Interestingly, 8-Gin and VER can obviously improve pathological damage of the heart.

### 3.3 | Effects of 8-Gin on cardiac oxidative stress and calcium concentration

Figure 3A suggested that compared to the CON group, the production of ROS was increased in the ISO group. Surprisingly, the fluorescence intensity of ROS was significantly weakened in the 8-Gin and VER groups. In addition, the activities of SOD, CAT, and GSH in serum decreased in the ISO group ( $p < .01$ ) as shown in Figure 3B,D,E, while the content of MDA in the ISO group showed an increase when compared with the CON group ( $p < .01$ ) as shown in Figure 3C. After treatment with 8-Gin and VER, SOD, CAT, and GSH activities were observably enhanced, and the level of MDA had distinctly decreased in contrast to the ISO group ( $p < .01$ ). As shown in Figure 3F, the calcium concentration of heart tissue in the ISO group showed a marked increase ( $p < .01$ ) compared to the CON group. However, obvious declines in the 8-Gin group and VER group ( $p < .05$  or  $< .01$ ) were noted.

### 3.4 | Effects of 8-Gin on the expressions of Bcl-2, Bax, and Caspase-3

Figure 4B,E showed that Bax and Caspase-3 expression distinctly increased in the ISO group ( $p < .05$  or  $< .01$ ). Moreover, the ratio of Bax/Bcl-2 also increased markedly in the ISO group ( $p < .01$ ) as shown in Figure 4D. However, the expressions of Bcl-2 (Figure 4C)

in the ISO group were significantly decreased compared with the CON group ( $p < .01$ ). After 8-Gin and VER pretreatment, protein expression of Bax and Caspase-3 and the ratio of Bax/Bcl-2 were significantly down-regulated, while the level of Bcl-2 expression was noticeably up-regulated ( $p < .05$  or  $< .01$ ) in contrast to the ISO group.

### 3.5 | Effects of 8-Gin on MAPK signaling pathway

Figure 5A revealed that the expression of the MAPK signaling pathway showed a significant increase compared to the CON group in the ISO group. Pretreatment with 8-Gin, protein expression of p38, JNK, and ERK1/2 was reduced compared to the ISO group ( $p < .05$  or  $< .01$ ) (Figure 5B–D).

### 3.6 | Reduction of $I_{Ca-L}$ , cell shortening, and $Ca^{2+}$ transients by 8-Gin

#### 3.6.1 | Identification of $I_{Ca-L}$

In Figure 6, 10  $\mu$ M nifedipine (Nif), a specific LTCC antagonist,<sup>28</sup> obviously inhibited the currents, which illustrated that the recorded currents were  $Ca^{2+}$  currents ( $p < .01$ ). One-hundred micrometer  $NiCl_2$  as a specific T-type calcium channel blocker<sup>29</sup> had no effect on the currents, indicating that the recorded currents were not T-type  $Ca^{2+}$  currents. Another specific LTCCs blocker VER (10  $\mu$ M) almost eliminated the  $I_{Ca-L}$  ( $p < .01$ ), which further confirmed that the current recorded in ventricular myocytes was the L-type  $Ca^{2+}$  current.

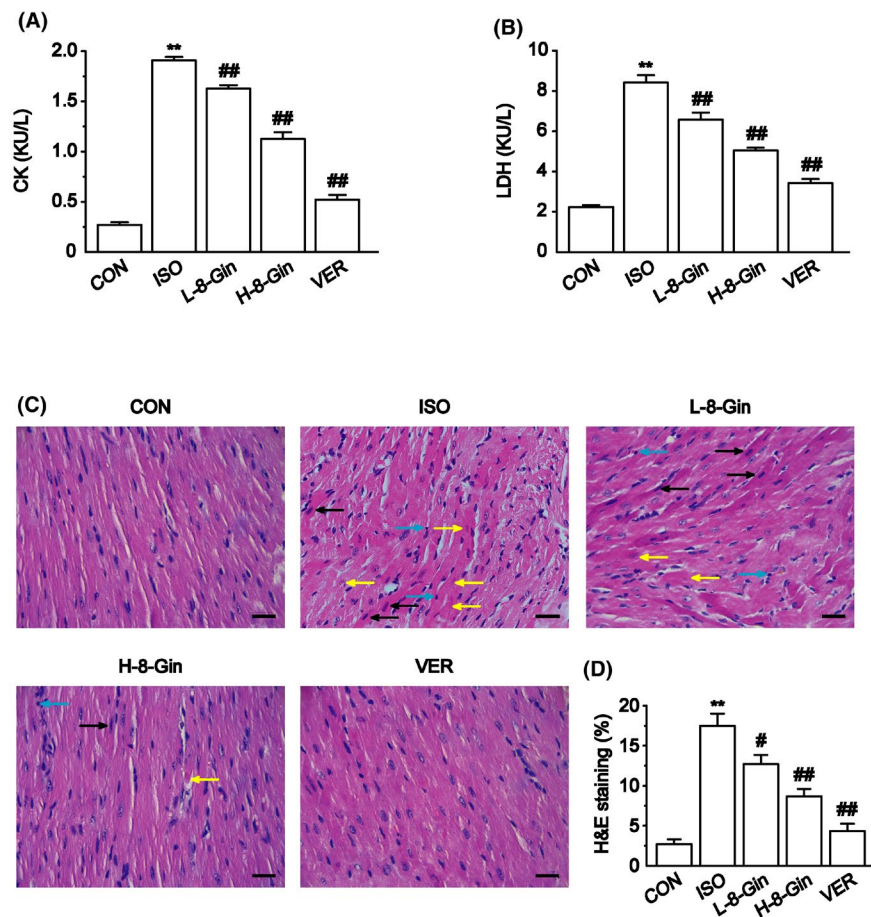
#### 3.6.2 | Effects of 8-Gin on $I_{Ca-L}$ in normal and ischemic ventricular myocytes

Figure 7A–F indicated that 8-Gin (30  $\mu$ M) caused a marked inhibition of the  $I_{Ca-L}$  of normal and ischemic ventricular myocytes with the inhibition rates of  $52.29\% \pm 2.20\%$  and  $49.76\% \pm 2.15\%$ , respectively ( $p < .01$ ). However, it could be observed that the  $I_{Ca-L}$  could be partially washed out by the external solution in Figure 7B,E. This result indicated the effects of 8-Gin on  $I_{Ca-L}$  were reversible.

#### 3.6.3 | Dose-dependent effects of 8-Gin on $I_{Ca-L}$

Figure 7G illustrated that the changes in the  $I_{Ca-L}$  as shown on the representative trace recordings after sequential exposure to different 8-Gin concentrations (1, 3, 10, 30, and 100  $\mu$ M) and 10  $\mu$ M VER. Moreover, Figure 7H displayed the time dependency of 8-Gin effects on the  $I_{Ca-L}$ . The inhibition rates of different 8-Gin concentrations were  $7.15\% \pm 1.20\%$ ,  $12.67\% \pm 1.37\%$ ,  $24.75\% \pm 1.15\%$ ,  $48.80\% \pm 1.71\%$ , and  $74.20\% \pm 1.25\%$ , respectively. The data





**FIGURE 2** Effects of 8-Gin on myocardial enzymes and histopathology. (A, B) Effects of 8-Gin on the levels of CK and LDH. CK and LDH activities were measured using commercial detection kits. Data are presented as the mean  $\pm$  SEM ( $n = 6$ ). \*\* $p < .01$  compared with the CON group; ## $p < .01$  compared with the ISO group. Statistical analyses were performed using one-way ANOVA followed by the Bonferroni correction. (C) Effects of 8-Gin on cardiac histopathology. Representative sections were obtained from the myocardial tissue of CON, ISO, L-8-Gin, H-8-Gin, and VER groups. Magnification,  $\times 400$ ; scale bar = 50  $\mu\text{m}$ . Histopathological changes are indicated by black (apoptosis), yellow (myocardial necrosis), and blue (inflammatory cell infiltration) arrows. (D) The area of myocardial injury in each group was calculated by Image-Pro Plus software. Randomly selected six visual fields per section and measured the positive area. Data are presented as the mean  $\pm$  SEM ( $n = 6$ ). \*\* $p < .01$  compared with the CON group; # $p < .05$  and ## $p < .01$  compared with the ISO group. Statistical analyses were performed using one-way ANOVA followed by the Bonferroni correction

clarified that 8-Gin could reduce  $I_{\text{Ca-L}}$  in a dose-dependent manner. Figure 7I indicated that the half-maximal inhibitory concentration ( $\text{IC}_{50}$ ) of 8-Gin was  $31.22 \pm 5.01 \mu\text{M}$ .

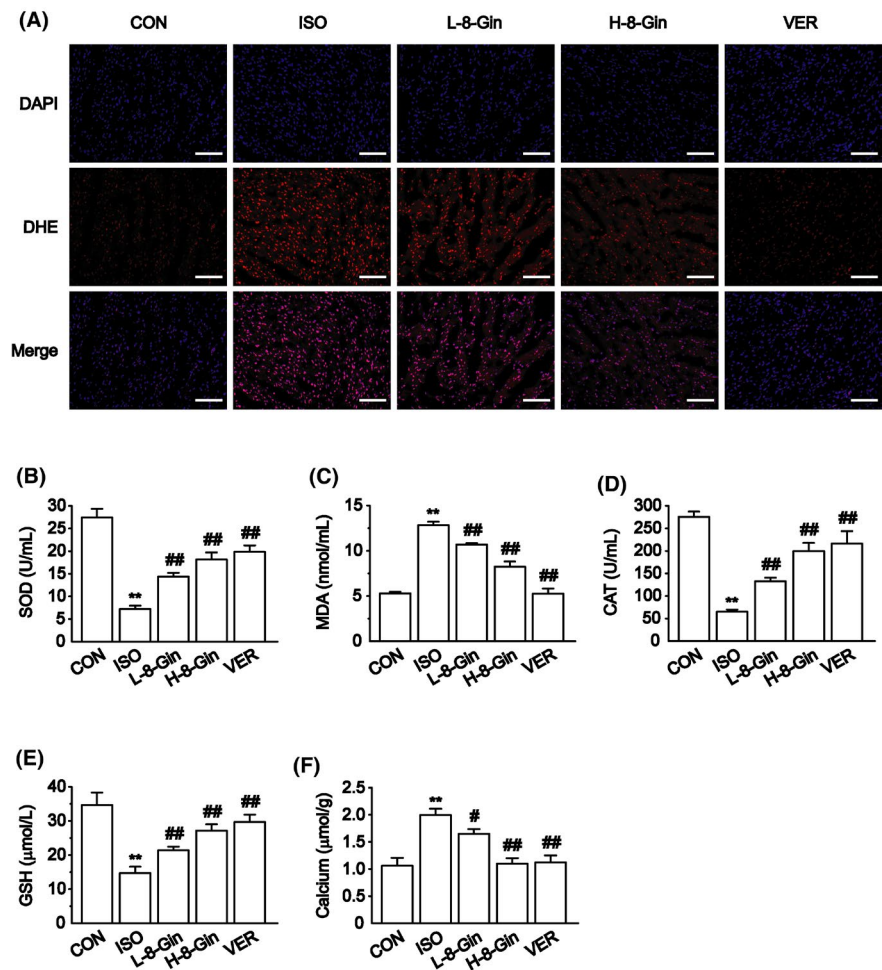
### 3.6.4 | Effects of 8-Gin on current-voltage (I-V) relationship of $I_{\text{Ca-L}}$

Current-voltage (I-V) curves for voltage-dependent activation of  $I_{\text{Ca-L}}$  were established from the active protocol (Figure 8B). Figure 8A showed representative trace recordings in the absence and presence of 8-Gin (3, 10, and 30  $\mu\text{M}$ ) and VER (10  $\mu\text{M}$ ). Figure 8C depicted the normalized I-V curves of  $I_{\text{Ca-L}}$  with 8-Gin (3, 10, and 30  $\mu\text{M}$ ). However, the I-V relationship and reversal potential of  $I_{\text{Ca-L}}$  did not show a marked change.

### 3.6.5 | Effects of 8-Gin on steady-state activation and inactivation of $I_{\text{Ca-L}}$

As shown in Figure 9, the effects of different doses of 8-Gin (3 and 10  $\mu\text{M}$ ) on the voltage dependence of steady-state activation and inactivation of  $I_{\text{Ca-L}}$  were recorded. The values at  $V_{1/2}$  and the slope factor ( $k$ ) of the normalized activation conductance curves were  $-12.78 \pm 0.37 \text{ mV}/4.60 \pm 0.32$  for CON condition,  $-14.26 \pm 0.32 \text{ mV}/5.03 \pm 0.27$  for 3  $\mu\text{M}$  8-Gin, and  $-14.67 \pm 0.36 \text{ mV}/5.54 \pm 0.31$  for 10  $\mu\text{M}$  8-Gin. The values at  $V_{1/2}$  and the slope factor ( $k$ ) of the normalized inactivation conductance curves were  $-27.33 \pm 0.41 \text{ mV}/4.41 \pm 0.36$  for CON condition,  $-26.76 \pm 0.30 \text{ mV}/3.97 \pm 0.24$  for 3  $\mu\text{M}$  8-Gin, and  $-29.89 \pm 0.11 \text{ mV}/4.46 \pm 0.12$  for 10  $\mu\text{M}$  8-Gin.

**FIGURE 3** Effects of 8-Gin on oxidative stress and calcium concentration. (A) Production of ROS was measured in frozen heart tissues with a dihydroethidium probe. Magnification  $\times 200$ ; scale bar = 100  $\mu\text{m}$ . Randomly selected three visual fields per section. (B–E) Effects of 8-Gin on MDA concentration and SOD, CAT, and GSH activities. MDA concentration and SOD, CAT, and GSH activities were measured using commercial detection kits. Data are presented as the mean  $\pm$  SEM ( $n = 6$ ). \*\* $p < .01$  compared with the CON group; ## $p < .01$  compared with the ISO group. (F) Effects of 8-Gin on calcium concentration in myocardium. The calcium concentration was measured using commercial detection kits. Data are presented as the mean  $\pm$  SEM ( $n = 6$ ). \*\* $p < .01$  compared with the CON group; # $p < .05$  and ## $p < .01$  compared with the ISO group. Statistical analyses were performed using one-way ANOVA followed by the Bonferroni correction



### 3.6.6 | Effects of 8-Gin on cardiomyocytes contraction and time parameters

Figure 10A indicated that 8-Gin caused a marked inhibition in cell shortening. Figure 10B showed the representative cell shortening recordings before and after treatment with 8-Gin (30  $\mu\text{M}$ ). And the inhibition rates of 8-Gin were  $46.19\% \pm 2.14\%$  for 30  $\mu\text{M}$  and  $89.20\% \pm 3.32\%$  for 100  $\mu\text{M}$  ( $p < .05$ ) as shown in Figure 10C. The time to 50% of the peak (TP) and the time to 50% of the baseline (TR) represent the parameters of the speed of myocyte contractions or  $\text{Ca}^{2+}$  elevation and cellular relaxation or  $\text{Ca}^{2+}$  reuptake, respectively. Figure 10D,E showed 30  $\mu\text{M}$  8-Gin decreased TP and TR ( $p < .05$ ).

### 3.6.7 | Effects of 8-Gin on cell $\text{Ca}^{2+}$ transients

Figure 11A revealed the changes in cell  $\text{Ca}^{2+}$  transients after exposure to absence and presence of 8-Gin (30  $\mu\text{M}$ ). The representative trace recordings of  $\text{Ca}^{2+}$  transients after treatment with 8-Gin (30  $\mu\text{M}$ ) were shown in Figure 11B. As shown in Figure 11C, the amplitudes of  $\text{Ca}^{2+}$  transients were reduced by  $20.61\% \pm 3.33\%$  and  $80.00\% \pm 3.54\%$  at the doses of 8-Gin (30 and 100  $\mu\text{M}$ ), respectively ( $p < .05$ ).

## 4 | DISCUSSION

Globally, MI has become the main outcome of many cardiovascular diseases in the world, which may pose a great threat to human health and the global economy.<sup>30</sup> Therefore, it is urgent to seek the potential preventive drugs to protect the heart against MI. Our study investigated that 8-Gin has a cardioprotective effect against ISO-induced MI. The underlying mechanisms were related to reducing oxidative stress, preventing cardiomyocyte apoptosis via inhibiting the MAPK signaling pathway, and suppressing  $\text{Ca}^{2+}$  overload through inhibiting the LTCCs.

ISO, a recognized drug to induce acute MI model in animals, results in myocardial injury mainly caused by oxygen free radical generation (oxidative stress) and  $[\text{Ca}^{2+}]_i$  concentration increase ( $\text{Ca}^{2+}$  overload).<sup>31,32</sup> The ISO-induced MI model was often recognized as a ubiquitous model for evaluating cardioprotective drugs.<sup>33–36</sup> High-dose subcutaneous injection of ISO can cause a significant reduction in the blood and oxygen supplies to the myocardium, which is responsible for serious damage to the structure and the functional changes seen on ECGs, and eventually leads to apoptosis and necrosis of myocardial cells.<sup>37</sup> It is similar to the changes caused by human MI.<sup>38</sup>

CK and LDH are two major myocardial marker enzymes. During MI, myocardial cells undergo alterations in metabolism, which

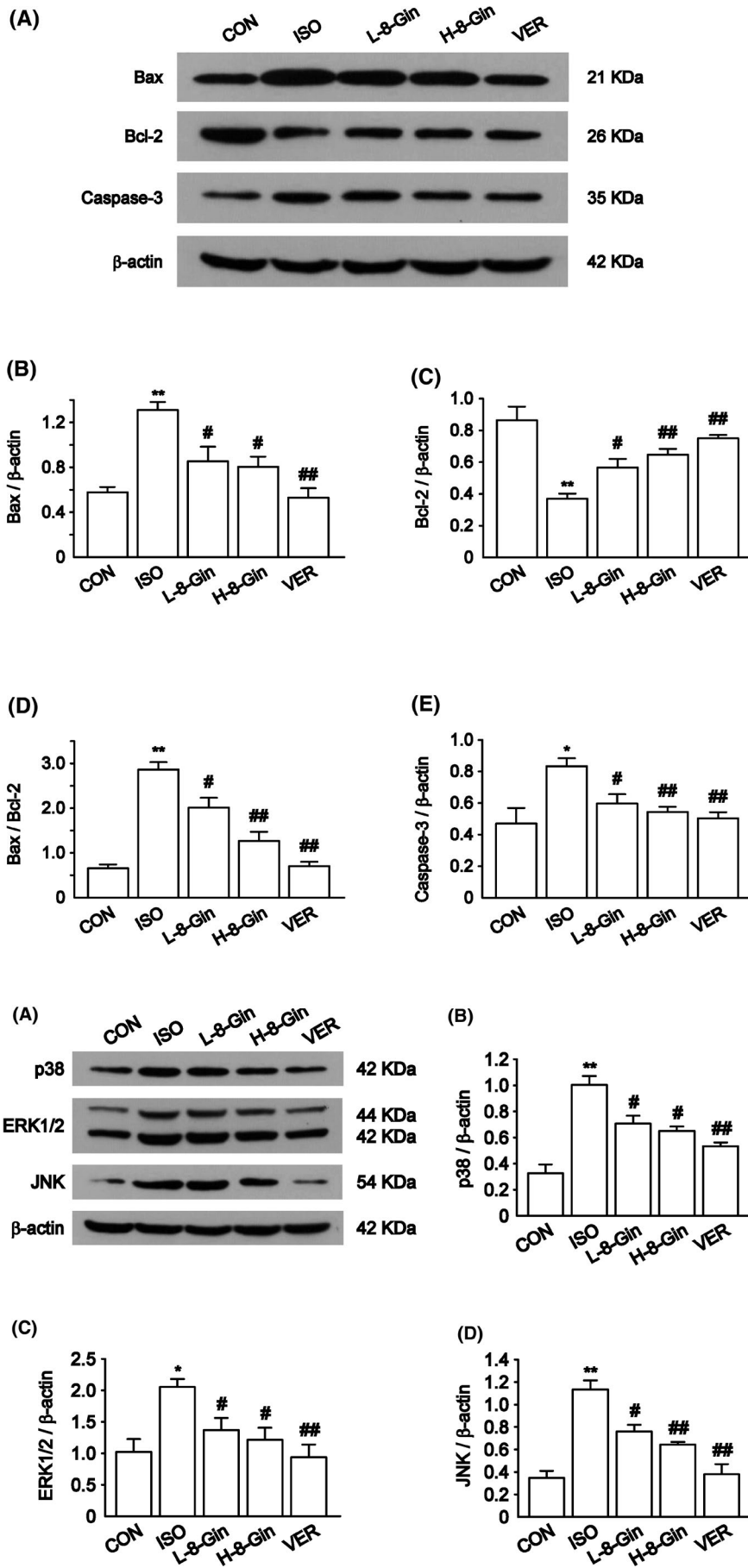


**FIGURE 4** Effects of 8-Gin on Bax, Bcl-2, and Caspase-3 proteins expression levels in rat heart. (A) Protein expression levels of Bax, Bcl-2, and Caspase-3 were measured by western blot analysis, and (B, C, E) intensity was normalized to  $\beta$ -actin. (D) The ratio of Bax and Bcl-2 protein expression levels. Data are presented as the mean  $\pm$  SEM ( $n = 3$ ). \* $p < .05$  and \*\* $p < .01$  compared with the CON group; # $p < .05$  and ## $p < .01$  compared with the ISO group. Statistical analyses were performed using one-way ANOVA followed by the Bonferroni correction

**FIGURE 5** Effects of 8-Gin on the MAPK signaling pathway-related proteins expression levels in rat heart. (A) Protein expression levels of p38, ERK1/2, and JNK were measured by western blot analysis and (B–D) intensity was normalized to  $\beta$ -actin. Data are presented as the mean  $\pm$  SEM ( $n = 3$ ). \* $p < .05$  and \*\* $p < .01$  compared with the CON group; # $p < .05$  and ## $p < .01$  compared with the ISO group. Statistical analyses were performed using one-way ANOVA followed by the Bonferroni correction



**FIGURE 6** Confirmation of  $I_{Ca-L}$  in cardiomyocytes. (A) Typical traces with the steady-state activation protocol before and after treatment of 10  $\mu$ M Nic, 100  $\mu$ M  $NiCl_2$ , and 10  $\mu$ M VER. (B) The statistical data showed 10  $\mu$ M Nic, 100  $\mu$ M  $NiCl_2$ , and 10  $\mu$ M VER on  $I_{Ca-L}$ . Data are presented as the mean  $\pm$  SEM ( $n = 6$  cells). \*\* $p < .01$ , compared with the CON group. Statistical analyses were performed using one-way ANOVA followed by the Bonferroni correction

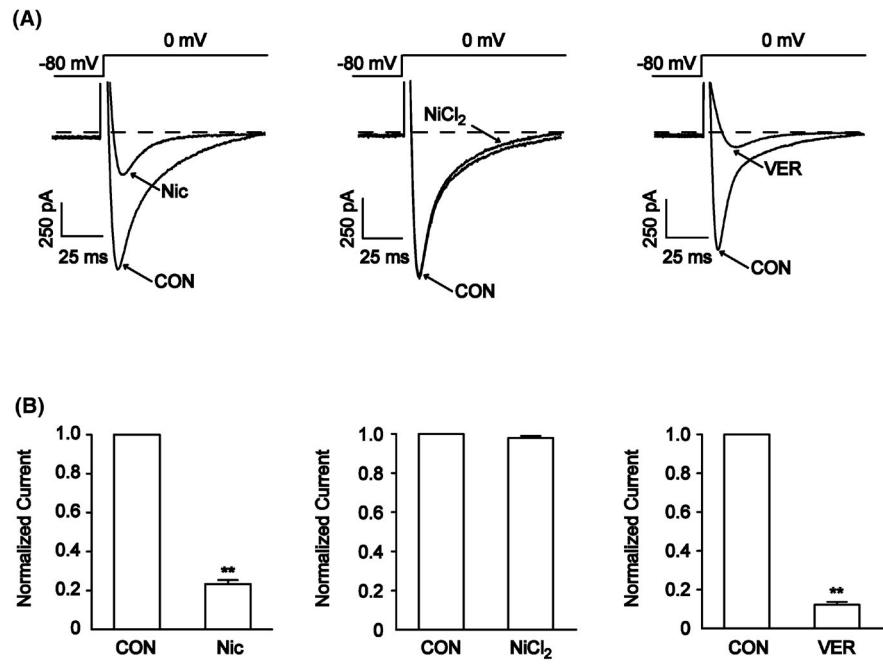
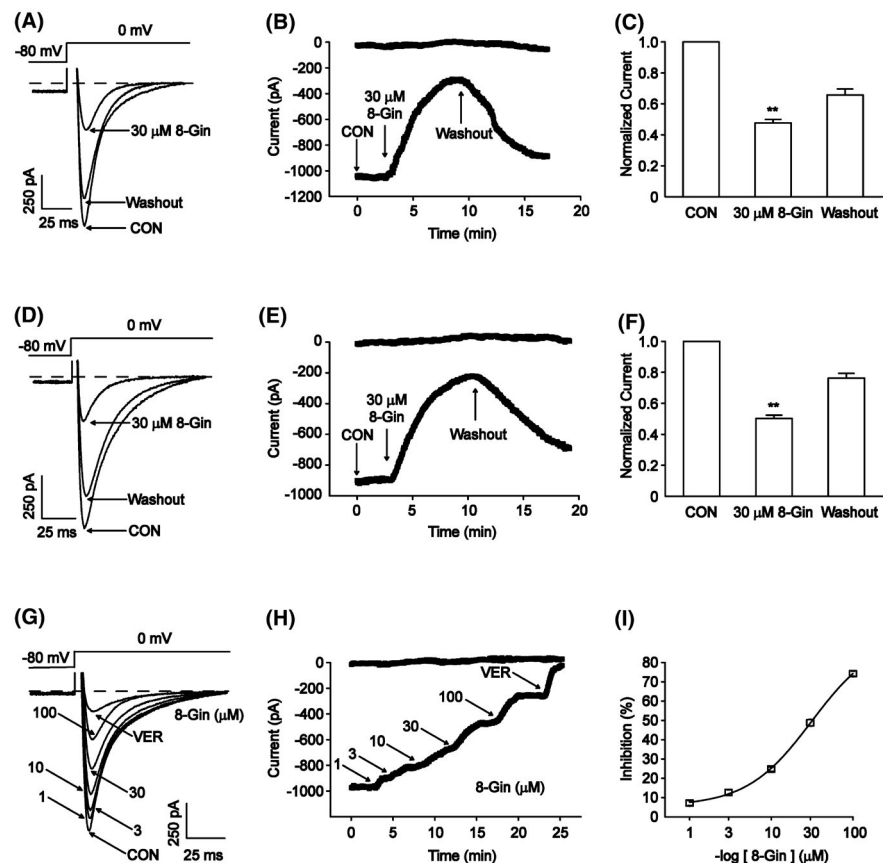


**FIGURE 7** Effects of 8-Gin on  $I_{Ca-L}$  in normal and ischemic rat ventricular myocytes. (A–C) Reversible effects of 8-Gin on  $I_{Ca-L}$  in normal rat ventricular myocytes. (D–F) Reversible effects of 8-Gin on  $I_{Ca-L}$  in ischemic rat ventricular myocytes. (A, D) Typical traces, (B, E) time constant of  $I_{Ca-L}$ , and (C, F) statistical results were recorded by the conditions of CON, 8-Gin (30  $\mu$ M), and washout. Data are presented as the mean  $\pm$  SEM ( $n = 6$  cells). \*\* $p < .01$ , compared with the CON group. (G) Typical traces and (H) time constant of  $I_{Ca-L}$  were continuously measured under the conditions of CON and 1, 3, 10, 30, and 100  $\mu$ M 8-Gin and 10  $\mu$ M VER. (I) The percent inhibitory of  $I_{Ca-L}$  by 8-Gin (1–100  $\mu$ M) was represented by dose–response curves. Data are presented as the mean  $\pm$  SEM ( $n = 6$  cells). Statistical analyses were performed using one-way ANOVA followed by the Bonferroni correction



causes a sharp increase in enzyme activity in the blood and further aggravates damage to cardiomyocytes.<sup>39</sup> Therefore, when MI occurs, detecting the activities of these two enzymes in serum can determine myocardial injury degree. In the present study, we found that CK and LDH levels in serum have both increased in the ISO group (Figure 2A,B). Moreover, we observed the histomorphological

changes in the heart and discovered that myocardial cells were arranged in a disorderly manner, apoptosis and necrosis occurred, cell nucleus was reduced, and inflammatory cell infiltrated in the ISO group (Figure 2C). In addition, ISO significantly caused J-point elevation and an increase in heart rate (Table 1). The clinical manifestations of MI are mostly ST segment elevation of ECG, which

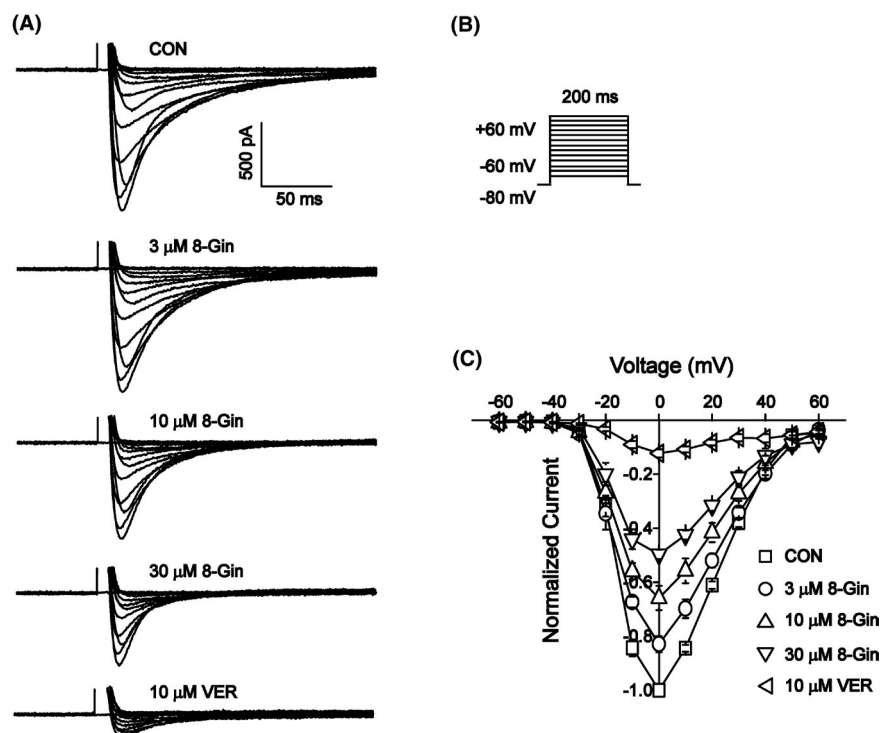


**FIGURE 8** Effects of 8-Gin on I-V relationship of  $I_{Ca-L}$ . (A) Representative  $I_{Ca-L}$  recordings with the steady-state activation protocol before and after application of 8-Gin (3, 10, and 30  $\mu$ M) or VER (10  $\mu$ M). (B) The active protocol of I-V relationship of  $I_{Ca-L}$ . (C) The I-V relationship of  $I_{Ca-L}$  in rat ventricular myocytes in CON, 8-Gin (3, 10, and 30  $\mu$ M), or VER (10  $\mu$ M). Data are presented as the mean  $\pm$  SEM ( $n = 6$  cells). Statistical analyses were performed using one-way ANOVA followed by the Bonferroni correction

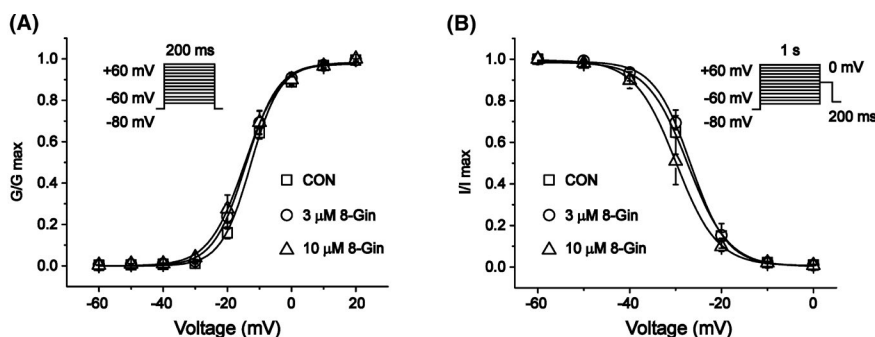


**FIGURE 9** Effects of 8-Gin on steady-state activation and inactivation of  $I_{Ca-L}$ . (A) Steady-state activation curves of normalized conductance values from the I-V curves in the CON and 3 and 10  $\mu$ M 8-Gin. (B) Normalized steady-state inactivation of  $I_{Ca-L}$  in the CON and 3 and 10  $\mu$ M 8-Gin. Data are presented as the mean  $\pm$  SEM ( $n = 6$  cells). Statistical analyses were performed using one-way ANOVA followed by the Bonferroni correction

reflects the degree of MI injury.<sup>40-42</sup> It is one of the most important indicators to evaluate the degree of MI. These results indicated ISO-induced MI injury, and we successfully established ISO-induced MI experimental model in rats. However, 8-Gin caused a reduction in the activities of CK and LDH compared with the ISO group (Figure 2A,B). Furthermore, we also observed abnormal morphological changes and the structure of the ischemic myocardium were alleviated to varying degrees (Figure 2C,D). Above results demonstrated that 8-Gin has a protective effect on ISO-induced MI.

Oxidative stress appears to be one of the important pathological mechanisms of MI. If MI does occur, the oxidative stress reaction would be accelerated, thus, causing a large accumulation of oxygen free radicals, ROS production, and  $Ca^{2+}$  overload, which would lead to aggravated myocardial injury and even cause cardiocyte apoptosis.<sup>14,43</sup> SOD, CAT, and GSH, as important antioxidant

enzymes, can effectively eliminate oxygen free radicals and prevent ROS generation so as to protect myocardial tissue. In addition, excessive production of oxygen free radicals can cause lipid peroxidation and further myocardial injury.<sup>44</sup> Our results showed that ROS production, MDA content, and calcium concentration were obviously increased in the ISO group (Figure 3A,C,F), while the activities of SOD, CAT, and GSH were decreased in the ISO group compared with the CON group (Figure 3B,D,E). After treatment with 8-Gin, ROS generation, MDA content, and calcium concentration declined, while SOD, CAT, and GSH levels significantly increased, indicating 8-Gin could ameliorate ISO-induced oxidative stress damage.

Previous studies have reported that ISO induced oxidative stress and activated MAPK signaling pathway in rats with acute ISO-induced MI.<sup>45,46</sup> Studies suggested that p38 MAPK can lead to

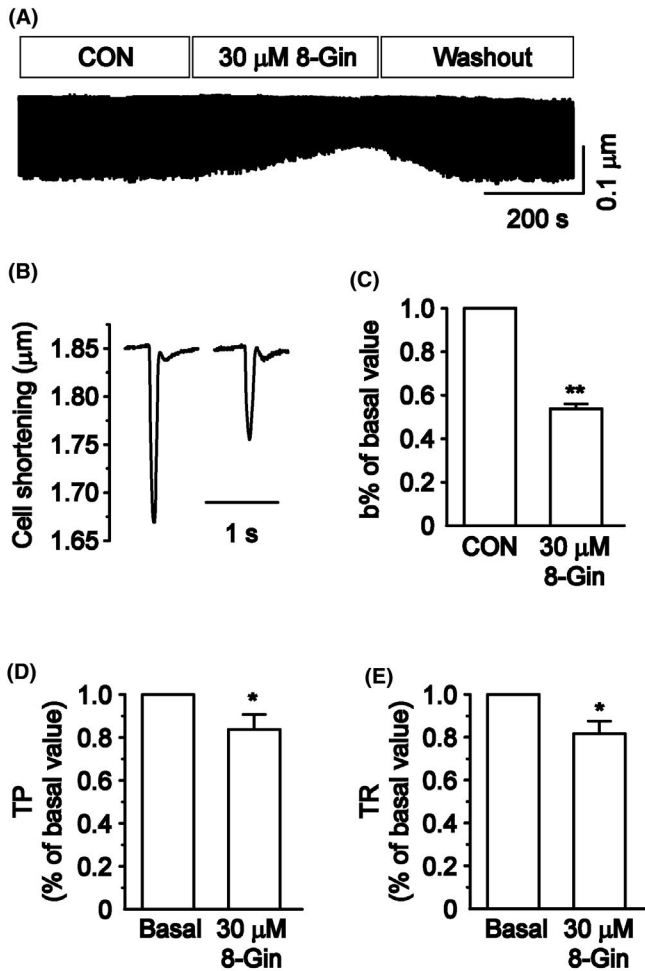


**FIGURE 10** Effects of 8-Gin on  $\text{Ca}^{2+}$  contraction and time parameters in rat ventricular myocytes. (A) The course of ventricular myocytes contraction recorded under CON conditions, 30  $\mu\text{M}$  8-Gin, and washout. (B) Single representative trace of cell shortening recorded in control conditions and 30  $\mu\text{M}$  8-Gin. (C) Summary results of CON and 30 and 100  $\mu\text{M}$  8-Gin. (D–E) Summary results of TP and TR in the CON and 30  $\mu\text{M}$  8-Gin. Data are presented as the mean  $\pm$  SEM ( $n = 6$  cells). \* $p < .05$  and \*\* $p < .01$  compared with the CON group. Statistical analyses were performed using one-way ANOVA followed by the Bonferroni correction

myocardial injury, mainly by aggravating inflammation, metabolic disorders, and apoptosis promotion<sup>46</sup>; the JNK pathway is mainly involved in apoptosis and the activity of ERK1/2 and can be inhibited by p38 and JNK.<sup>47</sup> Previous studies suggested that the MAPK pathway and JNK signaling cascades have been involved in hypoxia-induced H9c2 cell apoptosis.<sup>48,49</sup> In addition, there was evidence that ERK1/2 activation played a role in Bcl-2 family-mediated cell apoptosis induced by doxorubicin in cardiomyocytes.<sup>50</sup> Bcl-2 and Bax are both important members of the Bcl-2 protein family that is involved in the process of apoptosis. In the process of apoptosis, Caspase-3, a member of the cysteinyl aspartate-specific protease family, plays a crucial role. Caspase-3 can be activated by the Bcl-2 protein family.<sup>51</sup> Liu et al. found that carnosic acid could inhibit the apoptosis in H9c2 cardiomyocytes via down-regulation of Caspase-3

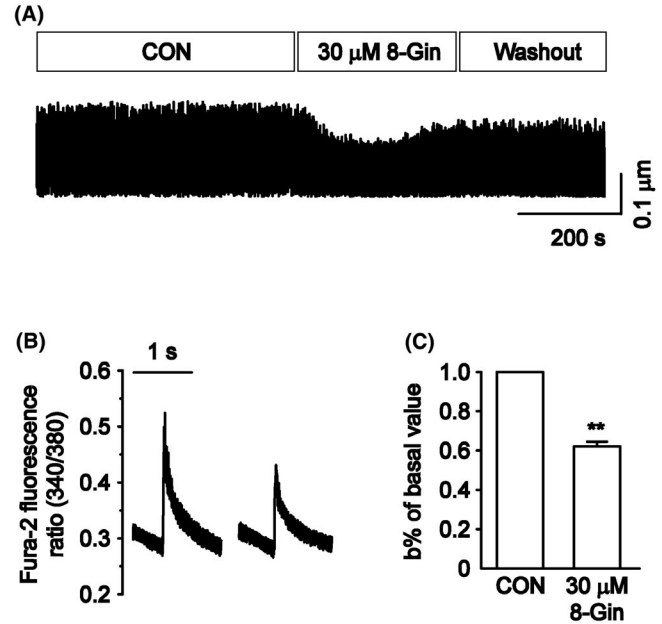


**FIGURE 11** Effects of 8-Gin on  $\text{Ca}^{2+}$  transients in rat ventricular myocytes. (A)  $\text{Ca}^{2+}$  transients recorded under CON and 30  $\mu\text{M}$  8-Gin in rat ventricular myocytes. (B) Single representative trace of  $\text{Ca}^{2+}$  transients recorded in the control condition and 30  $\mu\text{M}$  8-Gin. (C) Summary data of CON, and 30 and 100  $\mu\text{M}$  8-Gin. Data are presented as the mean  $\pm$  SEM ( $n = 6$  cells). \* $p < .05$ , compared with the CON group. Statistical analyses were performed using one-way ANOVA followed by the Bonferroni correction

and Bax expression and up-regulation of Bcl-2 expression.<sup>52</sup> In our research, we found ISO caused a marked up-regulation of the protein expression of Bax, Caspase-3, p38, ERK1/2, and JNK and the ratio of Bcl-2/Bax (Figures 4 and 5), while down-regulated the expression of Bcl-2 (Figure 4C). The above results showed that ISO induced oxidative stress reaction and activated the MAPK signaling pathway, thus, causing cardiomyocyte apoptosis and, finally, leading to myocardial injury. After 8-Gin treatment, the above indexes were significantly ameliorated. The results demonstrated that 8-Gin may exert cardioprotective effects via inhibiting the MAPK pathway and further preventing cardiomyocyte apoptosis.

It is widely known that  $\text{Ca}^{2+}$  plays an important role in the excitation–contraction coupling in myocardium.<sup>53</sup> Therefore, the regulation of  $\text{Ca}^{2+}$  homeostasis in vivo is very essential for maintaining the normal cardiac psychological function.<sup>54</sup>  $\text{Ca}^{2+}$  influx triggers the opening of the sarcoplasmic reticulum, which results in the release of a large amount of  $\text{Ca}^{2+}$  from the SR and an increase in  $[\text{Ca}^{2+}]_i$ .<sup>55</sup> On the other hand, cardiac cell contraction is activated by the action potential-induced membrane depolarization and subsequent  $\text{Ca}^{2+}$  entry via LTCCs.<sup>29</sup> Previous studies have indicated that  $\text{Ca}^{2+}$  overload would increase cardiac mechanical contraction and further lead to myocardial dysfunction and even myocardial cell death.<sup>56,57</sup> Therefore, inhibiting LTCCs could lead to a decreased  $\text{Ca}^{2+}$  influx, slow myocardial contractility, and ameliorate cardiac function. In addition, the p38 MAPK pathway was reported to be also involved in the regulation of  $[\text{Ca}^{2+}]_i$ . Zhu et al. discovered

that the activation of p38 MAPK pathway caused  $\text{Ca}^{2+}$  overload during ischemia/reperfusion injury, whereas, after application of p38 MAPK pathway, inhibitor significantly attenuated  $\text{Ca}^{2+}$  overload and suppressed apoptosis.<sup>58</sup> In our study, we found that 8-Gin could not only reduce  $I_{\text{Ca-L}}$  in a concentrations-dependent manner at doses of 1, 3, 10, 30, and 100  $\mu\text{M}$  in normal ventricular myocytes (Figure 7G,H). The  $\text{IC}_{50}$  was  $31.22 \pm 5.01 \mu\text{M}$  (Figure 7I). Furthermore, 8-Gin also reduced the  $I_{\text{Ca-L}}$  in ischemic ventricular myocytes (Figure 7D–F). In addition, 8-Gin influenced the I–V relationship (Figure 8A) and steady-state activation and inactivation (Figure 9) of  $I_{\text{Ca-L}}$ . However, we did not find that 8-Gin could alter the reversal potential of  $I_{\text{Ca-L}}$  (Figure 8C). Beyond those findings, we also found that 8-Gin caused a significant suppression of ventricular myocytes contraction and  $\text{Ca}^{2+}$  transients (Figure 10A and Figure 11A). Surprisingly though, we realized that 8-Gin had the greater effect on cardiomyocytes contraction than  $\text{Ca}^{2+}$  transients. The possible explanation for this strange phenomenon was the particularly complex process of cell contraction, which was related to intracellular proteins (actin and myosin) besides  $[\text{Ca}^{2+}]_i$  concentration.<sup>59</sup> For this reason, we need to do more studies in order to explore more detailed mechanisms of the effect of 8-Gin on myocardial contraction in the future. TP and TR are the most representative time constants, which characterize the rate of myocardial contraction and relaxation separately. Our results indicated that 8-Gin caused a decrease in TP and TR (Figure 10D,E). Our experimental data indicate that 8-Gin could protect the heart, and the mechanism was related to reducing  $\text{Ca}^{2+}$  overload via LTCCs inhibition, which resulted in a decrease in cell contraction and reduction in myocardial oxygen consumption.

The limitations of this study should be discussed. There are many other ion channels on cardiomyocyte membrane, such as  $\text{K}^+$  channels,  $\text{Na}^+$  channels, and  $\text{Cl}^-$  channels, which also play important roles in regulating cardiac function. Therefore, the pharmacological selectivity of 8-Gin for other ion channels is also the focus of our future study.

In conclusion, our present results demonstrated that 8-Gin exerted a myocardial protective influence on ISO-induced and MI-induced injury. The potential mechanisms of 8-Gin against MI might be associated with reducing oxidative stress, inhibiting the MAPK signaling pathway, and further preventing cardiomyocyte apoptosis, in addition to suppressing LTCCs, thus, leading to a reduction in  $\text{Ca}^{2+}$  overload. This series of experimental results with 8-Gin may provide a new direction for the development of anti-MI drugs for clinical use in the future.

## ACKNOWLEDGMENTS

This present research was supported by the Project of Science and Technology Research Project of Hebei Province (No. BJ2020002) and the Excellent Youth Program of Hebei University of Chinese Medicine (No. YQ2020003).

## DISCLOSURE

The authors declare that they have no financial conflicts of interest.

## AUTHORS' CONTRIBUTIONS

Participated in research design: Y. C. X., M. Q. Z., and L. C. Conducted experiments: Y. C. X., M. Q. Z., B. Z., and Y. Y. Z. Performed data analysis: Y. C. X., M. Q. Z., X. C., Y. L., and Z. L. L. Wrote or contributed to the writing of the manuscript: Y. C. X., X. H., and L. C.

## DATA AVAILABILITY STATEMENT

The datasets analyzed during the current study are available from the corresponding author on reasonable request.

## ORCID

Li Chu  <https://orcid.org/0000-0002-6301-2709>

## REFERENCES

1. Surh YJ, Lee E, Lee JM. Chemoprotective properties of some pungent ingredients present in red pepper and ginger. *Mutat Res*. 1998;402:259-267.
2. Liu Y, Liu JC, Zhang YQ. Research progress on chemical constituents of *Zingiber officinale* Roscoe. *Biomed Res Int*. 2019;2019:5370823.
3. Dugasani S, Pichika MR, Nadarajah VD, Balijepalli MK, Tandra S, Korlakunta JN. Comparative antioxidant and anti-inflammatory effects of [6]-gingerol, [8]-gingerol, [10]-gingerol and [6]-shogaol. *J Ethnopharmacol*. 2010;127:515-520.
4. Borcan F, Chirita-Emandi A, Andreescu NI, et al. Synthesis and preliminary characterization of polyurethane nanoparticles with ginger extract as a possible cardiovascular protector. *Int J Nanomedicine*. 2019;14:3691-3703.
5. Kobayashi M, Ishida Y, Shoji N, Ohizumi Y. Cardiogenic action of [8]-gingerol, an activator of the  $\text{Ca}^{++}$ -pumping adenosine triphosphatase of sarcoplasmic reticulum, in guinea pig atrial muscle. *J Pharmacol Exp Ther*. 1988;246:667-673.
6. Zhang S, Wang W, Wu X, Zhou X. Regulatory roles of circular RNAs in coronary artery disease. *Mol Ther Nucleic Acids*. 2020;21:172-179.
7. Savchenko AS, Borissoff JI, Martinod K, et al. VWF-mediated leukocyte recruitment with chromatin decondensation by PAD4 increases myocardial ischemia/reperfusion injury in mice. *Blood*. 2014;123:141-148.
8. Sun LP, Wang K, Xu X, Ge MM, Chen YF, Hu FL. Potential protective effects of bioactive constituents from Chinese propolis against acute oxidative stress induced by hydrogen peroxide in cardiac H9c2 cells. *Evid Based Complement Alternat Med*. 2017;2017:7074147.
9. Gao XF, Zhou Y, Wang DY, Lew KS, Richards AM, Wang P. Urocortin-2 suppression of p38-MAPK signaling as an additional mechanism for ischemic cardioprotection. *Mol Cell Biochem*. 2015;398:135-146.
10. Li DY, Tao L, Liu H, Christopher TA, Lopez BL, Ma XL. Role of ERK1/2 in the anti-apoptotic and cardioprotective effects of nitric oxide after myocardial ischemia and reperfusion. *Apoptosis*. 2006;11:923-930.
11. Shimada K, Nakamura M, Ishida E, Kishi M, Konishi N. Roles of p38- and c-jun NH2-terminal kinase-mediated pathways in 2-methoxyestradiol-induced p53 induction and apoptosis. *Carcinogenesis*. 2003;24:1067-1075.
12. Yue JC, Lopez JM. Understanding MAPK signaling pathways in apoptosis. *Int J Mol Sci*. 2020;21:2346. <http://doi.org/10.3390/ijms21072346>.
13. Green DR, Llamby F. Cell death signaling. *Cold Spring Harb Perspect Biol*. 2015;7:a006080.
14. Syeda MZ, Fasaie MB, Yue ER, et al. Anthocyanidin attenuates myocardial ischemia induced injury via inhibition of ROS-JNK-Bcl-2 pathway: new mechanism of anthocyanidin action. *Phytother Res*. 2019;33:3129-3139.

15. Sun G-B, Sun H, Meng X-B, et al. Aconitine-induced  $\text{Ca}^{2+}$  overload causes arrhythmia and triggers apoptosis through p38 MAPK signaling pathway in rats. *Toxicol Appl Pharmacol*. 2014;279:8-22.
16. Zhao ZF, Zheng B, Li JH, et al. Influence of crocetin, a natural carotenoid dicarboxylic acid in saffron, on L-type  $\text{Ca}^{2+}$  current, intracellular  $\text{Ca}^{2+}$  handling and contraction of isolated rat cardiomyocytes. *Biol Pharm Bull*. 2020;43:1367-1374.
17. Jennings RB. Historical perspective on the pathology of myocardial ischemia/reperfusion injury. *Circ Res*. 2013;113:428-438.
18. He F, Wu Q, Xu B, et al. Suppression of Stim1 reduced intracellular calcium concentration and attenuated hypoxia/reoxygenation induced apoptosis in H9c2 cells. *Biosci Rep*. 2017;37:BSR20171249.
19. Cingolani HE, Ennis IL. Sodium-hydrogen exchanger, cardiac overload, and myocardial hypertrophy. *Circulation*. 2007;115:1090-1100.
20. Song N, Ma J, Meng X-W, et al. Heat shock protein 70 protects the heart from ischemia/reperfusion injury through inhibition of p38 MAPK signaling. *Oxid Med Cell Longev*. 2020;2020:3908641.
21. Song T, Chu X, Zhang X, et al. Bufalin, a bufanolide steroid from the parotoid glands of the Chinese toad, inhibits L-type  $\text{Ca}^{2+}$  channels and contractility in rat ventricular myocytes. *Fundam Clin Pharmacol*. 2017;31:340-346.
22. Han X, Li MY, Zhao ZF, et al. Mechanisms underlying the cardioprotection of total ginsenosides against myocardial ischemia in rats in vivo and in vitro: possible involvement of L-type  $\text{Ca}^{2+}$  channels, contractility and  $\text{Ca}^{2+}$  homeostasis. *J Pharmacol Sci*. 2019;139:240-248.
23. Lu J, Guan S, Shen X, et al. Immunosuppressive activity of 8-gingerol on immune responses in mice. *Molecules*. 2011;16:2636-2645.
24. Zhang F, Ma N, Gao YF, Sun LL, Zhang JG. Therapeutic effects of 6-Gingerol, 8-Gingerol, and 10-Gingerol on dextran sulfate sodium-induced acute ulcerative colitis in rats. *Phytother Res*. 2017;31:1427-1432.
25. Song Q, Chu XI, Zhang X, et al. Mechanisms underlying the cardioprotective effect of Salvianic acid A against isoproterenol-induced myocardial ischemia injury in rats: possible involvement of L-type calcium channels and myocardial contractility. *J Ethnopharmacol*. 2016;189:157-164.
26. Gao Y, Zhang K, Zhu F, et al. Salvia miltiorrhiza (Danshen) inhibits L-type calcium current and attenuates calcium transient and contractility in rat ventricular myocytes. *J Ethnopharmacol*. 2014;158:397-403.
27. Salem KA, Qureshi A, Ljubisavijevic M. Alloxan reduces amplitude of ventricular myocyte shortening and intracellular  $\text{Ca}^{2+}$  without altering L-type  $\text{Ca}^{2+}$  current, sarcoplasmic reticulum  $\text{Ca}^{2+}$  content or myofilament sensitivity to  $\text{Ca}^{2+}$  in Wistar rats. *Mol Cell Biochem*. 2010;340(1-2):115-123. <https://doi.org/10.1007/s11010-010-0408-7>
28. Ren Z, Ma J, Zhang P, et al. The effect of ligustrazine on L-type calcium current, calcium transient and contractility in rabbit ventricular myocytes. *J Ethnopharmacol*. 2012;144:555-561.
29. Liu T, Chu X, Wang H, et al. Crocin, a carotenoid component of Crocus sativus, exerts inhibitory effects on L-type  $\text{Ca}^{2+}$  current,  $\text{Ca}^{2+}$  transient, and contractility in rat ventricular myocytes. *Can J Physiol Pharmacol*. 2016;94:302-308.
30. Gu C, Li T, Jiang S, et al. AMP-activated protein kinase sparks the fire of cardioprotection against myocardial ischemia and cardiac ageing. *Ageing Res Rev*. 2018;47:168-175.
31. Mohanty I, Arya DS, Dinda A, Talwar KK, Joshi S, Gupta SK. Mechanisms of cardioprotective effect of Withania somnifera in experimentally induced myocardial infarction. *Basic Clin Pharmacol Toxicol*. 2004;94:184-190.
32. Tiwari R, Mohan M, Kasture S, Maxia A, Ballero M. Cardioprotective potential of myricetin in isoproterenol-induced myocardial infarction in Wistar rats. *Phytother Res*. 2009;23:1361-1366.
33. Kanter M, Aktas C, Erboğa M. Protective effects of quercetin against apoptosis and oxidative stress in streptozotocin-induced diabetic rat testis. *Food Chem Toxicol*. 2012;50:719-725.
34. Prince PS. A biochemical, electrocardiographic, electrophoretic, histopathological and in vitro study on the protective effects of (-) epicatechin in isoproterenol-induced myocardial infarcted rats. *Eur J Pharmacol*. 2011;671:95-101.
35. Mangali S, Bhat A, Dasari D, Sriram D, Dhar A. Inhibition of double stranded RNA dependent protein kinase (PKR) abrogates isoproterenol induced myocardial ischemia in vitro in cultured cardiomyocytes and in vivo in wistar rats. *Eur J Pharmacol*. 2021;906:174223.
36. Zhang X, Zhang J, Ji X, et al. A quantitative serum proteomic analysis helps to explore the comprehensive mechanism and identify serum biomarkers of Shengmai injection's effect on isoproterenol-induced myocardial ischemia in rats. *Front Pharmacol*. 2021;12:666429.
37. Kahn DS, Rona G, Chappel CI. Isoproterenol-induced cardiac necrosis. *Ann N Y Acad Sci*. 1969;156:285-293.
38. Karthikeyan K, Bai BR, Devaraj SN. Cardioprotective effect of grape seed proanthocyanidins on isoproterenol-induced myocardial injury in rat. *Int J Cardiol*. 2007;115:326-333.
39. Chen HG, Xu YF, Wang JZ, Zhao W, Ruan HH. Baicalin ameliorates isoproterenol-induced acute myocardial infarction through iNOS, inflammation and oxidative stress in rat. *Int J Clin Exp Pathol*. 2015;8(9):10139-10147. PMID: 26617721.
40. Herring N, Paterson DJ. ECG diagnosis of acute ischaemia and infarction: past, present and future. *QJM*. 2006;99:219-230.
41. Sclarovsky S, Mager A, Davidson E, Bassevich R, Rechavia E, Strasberg B. Classification of acute myocardial ischemia by electrocardiography. *Harefuah*. 1989;116:35-39.
42. Stoller M, Boehler A, Bloch N, et al. Effect of acute myocardial ischemia on inferolateral early repolarization. *Heart Rhythm*. 2020;17:922-930.
43. Dubois-Deruy E, Peugnet V, Turkieh A, Pinet F. Oxidative stress in cardiovascular diseases. *Antioxidants (Basel)*. 2020;9:864.
44. Buwa CC, Mahajan UB, Patil CR, Goyal SN. Apigenin attenuates beta-receptor-stimulated myocardial injury via safeguarding cardiac functions and escalation of antioxidant defence system. *Cardiovasc Toxicol*. 2016;16:286-297.
45. Higashi Y, Noma K, Yoshizumi M, Kihara Y. Endothelial function and oxidative stress in cardiovascular diseases. *Circ J*. 2009;73:411-418.
46. Zhang G, Kimura S, Nishiyama A, et al. Cardiac oxidative stress in acute and chronic isoproterenol-infused rats. *Cardiovasc Res*. 2005;65:230-238.
47. Yue T-L, Wang C, Gu J-L, et al. Inhibition of extracellular signal-regulated kinase enhances ischemia/reoxygenation-induced apoptosis in cultured cardiac myocytes and exaggerates reperfusion injury in isolated perfused heart. *Circ Res*. 2000;86:692-699.
48. Liou S-F, Hsu J-H, Chen Y-T, Chen I-J, Yeh J-L. KMUP-1 attenuates endothelin-1-induced cardiomyocyte hypertrophy through activation of heme oxygenase-1 and suppression of the Akt/GSK-3 $\beta$ , calcineurin/NFATc4 and RhoA/ROCK pathways. *Molecules*. 2015;20(6):10435-10449. <https://doi.org/10.3390/molecules200610435>
49. Xia P, Liu Y, Cheng Z. Signaling pathways in cardiac myocyte apoptosis. *BioMed Res Int*. 2016;2016:1-22.
50. Liu J, Mao W, Ding B, Liang CS. ERKs/p53 signal transduction pathway is involved in doxorubicin-induced apoptosis in H9c2 cells and cardiomyocytes. *Am J Physiol Heart Circ Physiol*. 2008;295:H1956-H1965.
51. He H, Xu J, Xu Y, et al. Cardioprotective effects of saponins from *Panax japonicus* on acute myocardial ischemia against oxidative stress-triggered damage and cardiac cell death in rats. *J Ethnopharmacol*. 2012;140:73-82.



52. Liu P, Dong J. Protective effects of carnosic acid against mitochondria-mediated injury in H9c2 cardiomyocytes induced by hypoxia/reoxygenation. *Exp Ther Med*. 2017;14:5629-5634.
53. Eisner DA, Caldwell JL, Kistamas K, Trafford AW. Calcium and excitation-contraction coupling in the heart. *Circ Res*. 2017;121:181-195.
54. Barry WH, Bridge JH. Intracellular calcium homeostasis in cardiac myocytes. *Circulation*. 1993;87:1806-1815.
55. Zima AV, Blatter LA. Redox regulation of cardiac calcium channels and transporters. *Cardiovasc Res*. 2006;71:310-321.
56. Bristow MR, Kantrowitz NE, Ginsburg R, Fowler MB. Beta-adrenergic function in heart muscle disease and heart failure. *J Mol Cell Cardiol*. 1985;17:41-52.
57. Chen XW, Zhang XY, Kubo H, et al.  $\text{Ca}^{2+}$  influx-induced sarcoplasmic reticulum  $\text{Ca}^{2+}$  overload causes mitochondrial-dependent apoptosis in ventricular myocytes. *Circ Res*. 2005;97:1009-1017.
58. Zhu S, Xu T, Luo Y, et al. Luteolin enhances sarcoplasmic reticulum  $\text{Ca}^{2+}$ -ATPase activity through p38 MAPK signaling thus improving rat cardiac function after ischemia/reperfusion. *Cell Physiol Biochem*. 2017;41:999-1010.
59. Adamcova M, Sterba M, Simunek T, Potacova A, Popelova O, Gersl V. Myocardial regulatory proteins and heart failure. *Eur J Heart Fail*. 2006;8:333-342. <http://doi.org/10.1016/j.ejheart.2005.09.007>

**How to cite this article:** Xue Y, Zhang M, Zheng B, et al. [8]-Gingerol exerts anti-myocardial ischemic effects in rats via modulation of the MAPK signaling pathway and L-type  $\text{Ca}^{2+}$  channels. *Pharmacol Res Perspect*. 2021;9:e00852. <https://doi.org/10.1002/prp2.852>